

Observation of Thermal Deuteron-Deuteron Fusion in Ion Tracks

K. Czerski¹, R. Dubey¹, A. Kowalska², G. Haridas Das¹, M. Kaczmarek¹, N. Targosz-Sleczka¹,
M. Valat¹

¹ Institute of Physics, University of Szczecin, 70-453 Szczecin, Poland

² Physics Department, Maritime University of Szczecin, 70-500 Szczecin, Poland

Abstract:

A direct observation of the deuteron-deuteron (DD) fusion reaction at thermal meV energies, although theoretically possible, is not succeeded up to now. The electron screening effect that reduces the repulsive Coulomb barrier between reacting nuclei in metallic environments by several hundreds of eV and is additionally increased by crystal lattice defects in the hosting material, leads to strongly enhanced cross sections which means that this effect might be studied in laboratories. Here we present results of the ${}^2\text{H}(d,p){}^3\text{H}$ reaction measurements performed on a ZrD_2 target down to the lowest deuteron energy in the center mass system of 675 eV, using an ultra-high vacuum accelerator system, recently upgraded to achieve high beam currents at very low energies. The experimental thick target yield, decreasing over seven orders of magnitude for lowering beam energies, could be well described by the electron screening energy of 340 eV, which is much higher than the value of about 100 eV for a defect free material. At the energies below 2.5 keV, a constant plateau yield value could be observed. As indicated by significantly increased energies of emitted protons, this effect can be associated with the thermal DD fusion. A theoretical model explains the experimental observations by creation of ion tracks induced in the target by projectiles, and a high phonon density which locally increases temperature above the melting point. The nuclear reaction rate taking into account recently observed DD threshold resonance agrees very well with the experimental data.

Nuclear reactions, when proceeding at very low energies in metallic environments, can be strongly enhanced by the electron screening effect resulting from reduction of the Coulomb barrier by surrounding, mainly conduction electrons. This effect has been observed for different reactions in direct^{1,2,3} and inverse kinematics⁴ and is of a large importance for dense astrophysical plasmas, where nuclear reaction rates can be increased by many orders of magnitude⁵. It is particularly strong in the deuteron-deuteron (DD) fusion reactions due to the relatively low Coulomb barrier of about 350 keV. The electron screening energy in these reactions, corresponding to the reduction of the Coulomb barrier, is larger than 100 eV for heavier metals and can be additionally enhanced by crystal lattice defects⁶, primarily due to vacancies decorated by oxygen⁷ atoms induced by hydrogen loading⁷.

On the other hand, recent accelerator studies on the DD fusion at very low energies strongly supports existence of a threshold resonance in ${}^4\text{He}$ placed at the excitation energy of about 23.8 MeV^{6,8}, which is responsible for a further enhancement of the reaction cross sections. Based on the first observation in the ${}^2\text{H}(d,p){}^3\text{H}$ reaction of interference effects between the narrow single particle $0+$ resonance and known broad resonances, a large partial width of this resonance for the internal e^+e^- pair production has been predicted⁸. A corresponding observation of emitted electron/positron energy spectra using a single Si detector could be presented in full agreement with theoretical predictions^{9,10}. New experiments performed with large volume NaI scintillation detector and HPGe detector also confirm emission of high energy bremsstrahlung as well a related excess of the positron annihilation line¹¹. A direct consequence of recent studies is that the fusion of two deuterons can take place with probabilities that enables its observation at thermal meV energies.

In this paper, we present new experimental results of the ${}^2\text{H}(d,p){}^3\text{H}$ reaction measured for the first time at the lowest deuteron beam energy of 1.25 keV applying a deuterated ZrD_2 target and the recently upgraded accelerator system with ultra-high vacuum at the University of Szczecin, Poland. For some other metallic targets, this reaction was previously studied at deuteron energies down to 3 keV and for PdO to 2.5 keV¹². The electron screening results in an exponential-like enhancement of reaction cross sections for lowering projectile energies due to change of the penetration factor which can be estimated for the s-wave partial wave as follows:

$$P_{scr}(E + U_e) = \sqrt{\frac{E_G}{E+U_e}} \exp\left(-\sqrt{\frac{E_G}{E+U_e}}\right), \quad (1)$$

where the screening energy U_e has been added to the center mass energy of reacting nuclei. The Gamow energy $E_G = 2(Z_1 Z_2 \pi / 137)^2 \mu$ is equal to 986 keV for the DD system (μ stay for the reduced mass). The reaction cross section can be then obtained using the expression for the penetration factor and the astrophysical S-factor $S(E)$:

$$\sigma_{scr}(E) = \frac{1}{\sqrt{E(E+U_e)}} S(E) \exp\left(-\sqrt{\frac{E_G}{E+U_e}}\right) = \frac{1}{\sqrt{E_G E}} S(E) P_{scr}(E + U_e) \quad (2)$$

The screening energy determined for the ${}^2\text{H}(d,p){}^3\text{H}$ reaction on deuterated Zr target varies between 100 and 400 eV depending on the crystal lattice vacancies of the hosting material^{6,8}. Whereas the lower value has been achieved for targets which were cleaned and amorphized by argon sputtering immediately before the measurements and agrees very well with theoretical predictions¹³, the higher screening energy has been observed during long term experiments, producing a large number of crystal vacancies⁷. This kind of the host

material structure leads to localization of conduction electrons and an increase of the effective electron mass resulting in an increase of the screening energy.

According to the formulas above, the cross section of the ${}^2\text{H}(d,p){}^3\text{H}$ reaction at $E=1$ keV should be enhanced compared to the bare nuclear case ($U_e = 0$) by a factor 4.1 or 109 depending on the screening energy equal to 100 or 400 eV. In both cases, determination of the screening energy would be much more exact if the measurements could be performed at the lowest possible energies. In the previous experiment⁶, $E=2.5$ keV could be reached, and the enhancement factor of about two could be observed.

Since the penetration factor for energies lower than the screening energy is constant, the cross section does not change strongly anymore. In that case, the single particle threshold resonance should dominate the astrophysical S-factor.

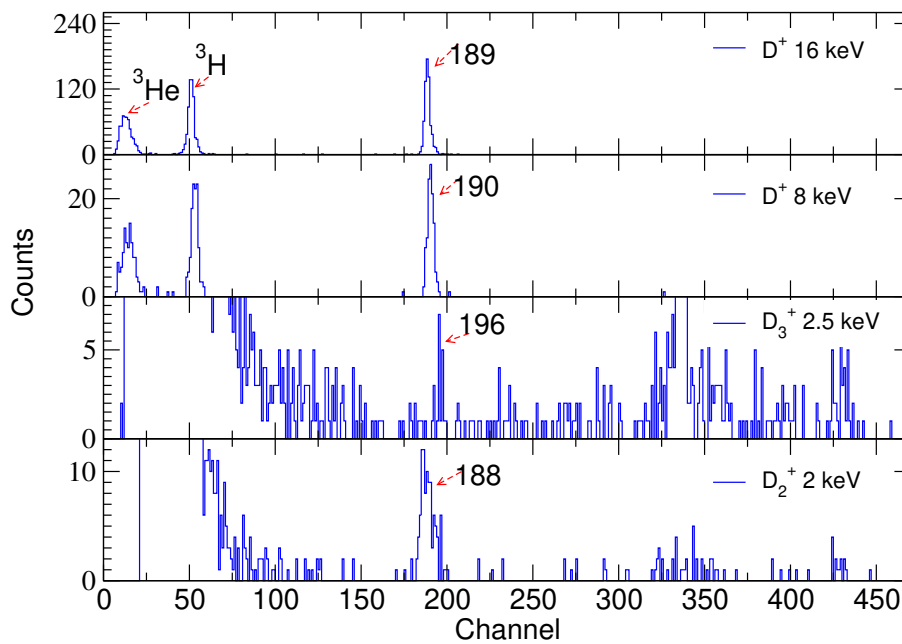


Fig. 1: Charged particle spectra of the ${}^2\text{H}(d,p){}^3\text{H}$ reaction at different deuteron energies, applying atomic and molecular deuterium beams. The numbers at the proton line show the channel number of the peak position (for comparison see Fig. 2b).

Low-energy thick target yield

Measurements at the lowest deuteron energies were possible due to use of a new deceleration lens system allowing to operate the ECR ion source at relatively high voltages with high beam currents. Atomic, D_2^+ and D_3^+ molecular ion beams have been applied to determine the thick target yield in a broad energy range of deuterons between 1.25 keV and 25 keV (0.613 keV and 12.5 keV in the center mass system). A low noise PIPS Si detector placed

backwards to the beam at 135° was used to detect the emitted charged particles. For details see the Method section. The experimental spectra and final results are presented in Fig. 1 and 2. The thick target yield can be calculated with the formula:

$$Y_{scr}(E) = N_0 \int_0^R \sigma_{scr}(E) dx = N_0 \int_0^E \frac{\sigma_{scr}(E)}{|dE/dx|} dE \approx \frac{2N_0 S(E)}{C\sqrt{E_G}} \exp\left(-\sqrt{\frac{E_G}{E+U_e}}\right) \quad (3)$$

where the stopping power function in the energy region studied is governed by the electronic stopping $|dE/dx| = C\sqrt{E}$ and N_0 stays for the deuteron number density.

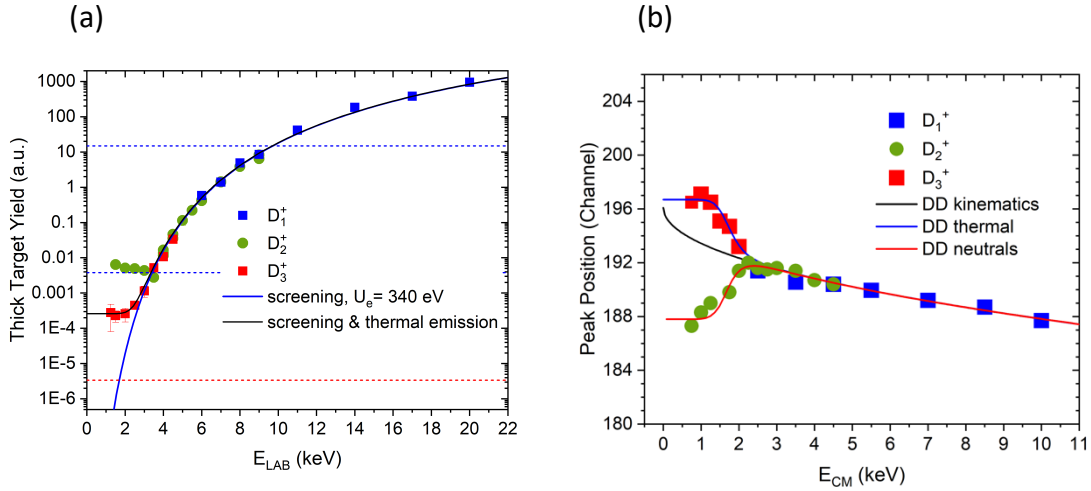


Fig. 2: **(a)** Thick target yield of the $2\text{H}(d,p)3\text{H}$ reaction. The blue full line corresponds the theoretical curve obtained for the screening energy $U_e=340\pm 30$ eV. The blue dashed lines show yield values obtained for the about 10^{-4} fraction of the neutralized D_2^+ beam (plateau) compared to the yield measured at 10 keV. The red dashed line corresponds to the expected yield for the neutralized D_3^+ beam. The yield plateau observed at the lowest energies is two orders of magnitude above. **(b)** Channel number of the proton peak position. At the lowest deuteron energies, the experimental data obtained with the D_3^+ beam can be described by thermal emission ($E=0$) (blue curve) and the fast-decreasing contribution corresponding to the screening curve from Fig. 3a. The neutral yield component for the D_2^+ beam can be described similarly by the red curve. High energy points follow the energies resulting from the kinematics of the $2\text{H}(d,p)3\text{H}$ reaction (black curve).

The experimental thick target yield decreases over the measured energy range by 7 orders magnitude following a theoretical curve assuming a constant astrophysical S-factor of 57 keV barn^{14} and the screening energy of 340 ± 30 eV. The smallest yield value was reached using the D_3^+ beam at the deuteron energies 2.0 keV corresponding to the cross section of about 100 pbarn. For lower deuteron energies, a constant plateau in the thick target yield was observed. Similar plateaus could also be detected at higher deuteron energies for D_1^+ and D_2^+ beams, clearly coming from a small number of ions neutralized at a distance of 1 m between electric steerers and the deceleration lenses and the target (see Fig. 6 in Methods section). The neutral atom contribution to both beams could be determined to be of about 10^{-4} by

comparison of the reaction yields measured with and without deceleration at the same ion source potential (see the blue horizontal dashed lines in Fig.2a). This number agrees with a theoretical estimation assuming the neutralization cross section¹⁵ of 10^{-15} cm² and the vacuum pressure of about 5×10^{-9} mbar in this part of beam line. Thus, a corresponding thick target yield induced by neutral deuteron atoms during the D_3^+ beam irradiation would be expected about two orders of magnitude below the observed plateau level (red horizontal dashed line in Fig. 2a), underlying its different origin.

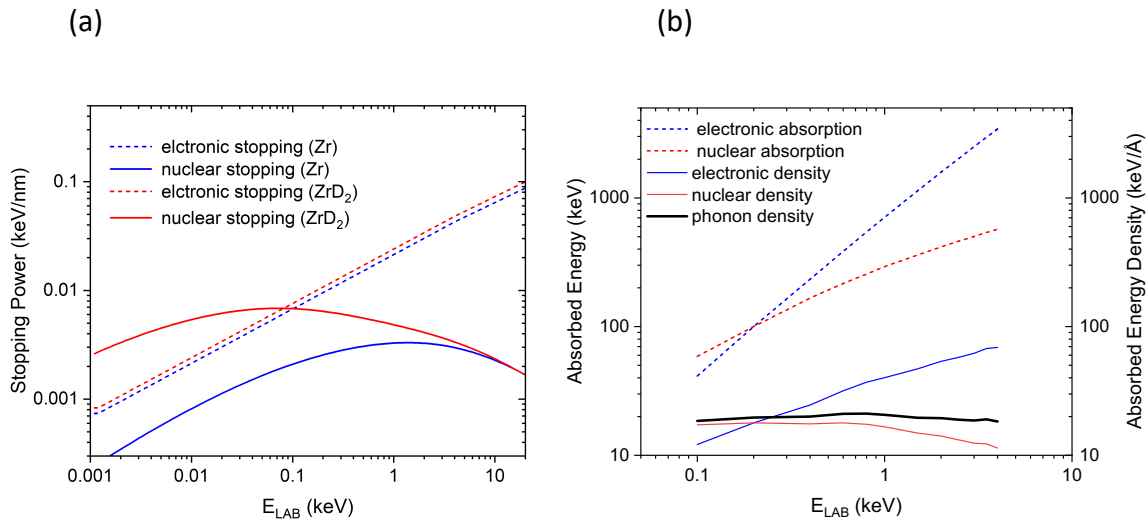


Fig. 3: **(a)** Nuclear and electronic stopping powers obtained for deuterons on Zr and ZrD₂ targets. **(b)** Deuteron beam energy absorbed by the ZrD₂ target due to nuclear and electronic stopping power (upper dashed curves). Electronic (full blue line) and nuclear (full red line) energy densities calculated as the corresponding absorbed energy divided by the range of the deuteron beam. The black line represents the total phonon density resulting from a sum of the nuclear energy density and 10% electronic energy densities, due to the electron-phonon coupling. The phonon density is almost constant at low deuteron energies. Calculations have been performed using the SRIM/TRIM code¹⁶.

The energy dependence of the position of the 3 MeV proton peak on the energy of the deuteron beam may provide a conclusive argument about the mechanism of the $^2\text{H}(d,p)^3\text{H}$ reaction. Since the Si detector was placed backwards from the beam, the proton peak should shift towards higher energies for lower deuteron energies (black curve in Fig. 2b). However, for the D_2^+ beam, we observe a completely different result – in the region of plateau, the proton peak energy moves to lower energies corresponding to values expected for neutral atoms which were not decelerated by the electric lens system in the front of the target chamber. The red curve in Fig. 2b, takes into account the constant neutral atom fraction in the D_2^+ beam and the ionic component which is responsible for the strongly decreasing thick target yield with the screening energy of 340 eV (blue curve in Fig. 2). In the case of irradiation with the D_3^+ beam, the proton peak position systematically takes much larger energy values, which excludes a significant contribution of neutral atoms. The corresponding proton peak

energies are higher than the kinematics curve predicts and can be explained as a superposition of the strongly decreasing screening part ($U_e=340$ eV) and the plateau contribution for which the energy of the center mass system is equal zero. This finding suggests that the protons are emitted from the ${}^2\text{H}(d,p){}^3\text{H}$ reaction occurring at thermal energies.

Thermal nuclear reaction rate

The theoretical cross section at thermal energies (lower than the screening energy) is governed by the 0^+ threshold resonance. The resonance energy is not exactly known and should be in the range⁸ of 1 eV. New measurements of the internal e^+e^- pair creation (IPC) in the DD reaction give an estimation for the total resonance width of 700 meV – with a branching ratio between IPC and the proton partial widths¹¹ of about 14. In this energy region, the penetration factor is constant and therefore, one could expect a plateau in the thick target yield for thermal energies. However, it should take place at much lower deuteron energy and at much lower level than observed in the present experiment. The experimental data suggest that plateau protons are emitted from the DD center mass system moving with energy close to zero. Thus, it is convincing to assume that the bombarding deuterons locally heat the deuterated Zr target to higher temperatures, which would enable a large number of deuterons to move within the crystal lattice and collide there with other deuterons. This mechanism would strongly increase the active volume of the target compared to the standard dynamics of the ion beam, being stopped in the target at a small range. Whereas the latter can be described by thick target yield proportional to the atomic number density, the former uses the nuclear reaction rates being characteristic for plasma physics with a quadratic dependence on N :

$$\begin{aligned} \mathcal{R}(T) &= \frac{N^2}{2} \langle \sigma v \rangle = \frac{N^2}{2} \frac{(8/\pi)^{1/2}}{\mu^{1/2}(kT)^{3/2}} \int_0^\infty \sigma(E) E \exp(-E/kT) dE = \\ &= N^2 \frac{16\pi^{3/2} \hbar^3 E_R^{1/2}}{\mu^2 a (kT)^{3/2}} (E_G/U_e)^{1/2} \exp[-(E_G/U_e)^{1/2}] \exp(-E_R/kT) \frac{\Gamma_p}{\Gamma} \end{aligned} \quad (4)$$

where the Maxwell-Boltzmann velocity distribution and the Breit-Wigner formula for the single-particle threshold resonance have been applied (see Method section). Γ_p and Γ stay for the partial proton and total resonance widths, respectively.

The nuclear reaction rates strongly depend on the screening energy and the temperature kT in the local target region where projectiles induce collision cascades with target atoms. At deuteron energies lower than several keV, the nuclear stopping mechanism increases with lowering deuteron energy oppositely to the electronic excitation of atoms (see Fig. 3a). The maximum of the nuclear stopping power for a ZrD₂ target is at 80 eV and is higher than for the electronic stopping. In the case of a pure metallic Zr target, the nuclear stopping power is lower and possesses a maximum at the deuteron energy 1.5 keV since the scattering

on heavier atoms results in a lower energy loss. Although, the atomic collision cascades have a small lateral size of a few fm, and their range reaches a value¹⁶ of 21 nm at 2 keV, the bombarding deuterons produce a strong lattice oscillation related to a high number of phonons. The total deuteron beam energy transferred to the target by means of electronic excitation and atomic collisions are presented in Fig. 3b. The latter increases very slowly with the deuteron energy. Assuming that the lateral size of the cascades does not strongly change with energy, the total beam energy transferred to cascades, divided by the beam range should correspond to the phonon density excited in this region. As can be seen in Fig. 3b, the phonon density slightly decreases now for deuteron energies between 0.5 - 4 keV. However, following the thermal spike models of ion tracks^{17,18} we can consider that about 10% of the projectile energy stored into the electronic excitation^{19,20} can be transferred to the lattice due to the electron-phonon coupling. Therefore, we finally can get an almost constant phonon density (Fig. 3b). The phonon energy in the ϵ -ZrD₂ phase amounts to about 100 meV and the related specific heat capacity is equal to 28 J/mol/K at room temperature²¹. According to the calculations performed with the TRIM code¹⁶, the ion track volume 1 nm² x 21 nm for the 2 keV beam transferring 0.420 keV to the collision cascades and 10% of the electronic excitation of 1600 eV would lead to the phonon density of about 580 eV/0.1 eV/21 nm³ = 280 phonons/nm³ and the initial temperature within the ion track of about 2540°K. This is above the Zr melting temperature of 2127°K, which explains the changes at the target surface observed after irradiation with the deuteron beam (see Fig. 4). The temperature within the ion track decreases during as it expands. According to the Bose-Einstein statistics, room temperature can be reached after 10⁻¹⁰ seconds for a volume of 1870 nm³ (74 nm² x 24.8nm) and a density 3.1 phonons/nm³. The average temperature during the ion track expansion amounts to about 980°K. Similar calculation can be performed for a 1 keV deuteron beam. Since the deuteron range and the absorption energy decrease to 11.4 nm and 364 eV, respectively, the initial phonon density slightly increases to the value of 319 phonons/nm³ and the average track temperature reaches 1080°K.

To estimate the nuclear reaction rates, the number of moving deuterons in the crystal lattice is necessary. It can be calculated with the relation describing the deuteron diffusion in Zr:

$$N = N_0 \exp(-E_A/kT) \quad (5)$$

where E_A is the activation energy equal to 40.1±0.8 kJ/mol (413 meV)²². The total number of moving deuterons within the ion track of a lifetime $\tau = 10^{-10}$ s can be then calculated as a product $N/N_0 \cdot V$, where V stays for the track volume. The corresponding values for the deuteron energies 1 and 2 keV are almost equal and amounts to 13.0 nm³ and 12.2 nm³, respectively. This result confirms that the phonon density within the ion track decides on the final free deuteron contribution to the thermal reaction rate. The reduction of the track range for the decreasing beam energy is compensated by the increase of the initial track

temperature. The detected number of emitted thermal protons per second can be achieved with the formula:

$$\mathcal{N}(T) = I \cdot V \cdot \tau \cdot \frac{\Omega}{4\pi} \cdot \mathcal{R}(T) \quad (6)$$

where the projectile current $I = 90 \mu\text{A}$ at deuteron energy 2 keV defines the number of tracks per second and Ω stays for the solid angle of the detector. For the average track temperature of 1080°K, track volume 1870 nm³, screening energy 340 eV and $\frac{\Omega}{4\pi} = 0.02$, we obtain one proton count per 10,000 s, which is about 3 times higher count rate than that observed in our experiment in the energy region of the yield plateau (see Fig. 2). In view of the many approximations we have made, this agreement between the theoretical prediction and experiment is very convincing, confirming both the absolute numbers and the energy independence of yield for beam energies below 2.5 keV. However, the uncertainty is relatively large and amounts to one to two orders of magnitude, mainly due to the uncertainty of the screening energy and electron-phonon coupling.

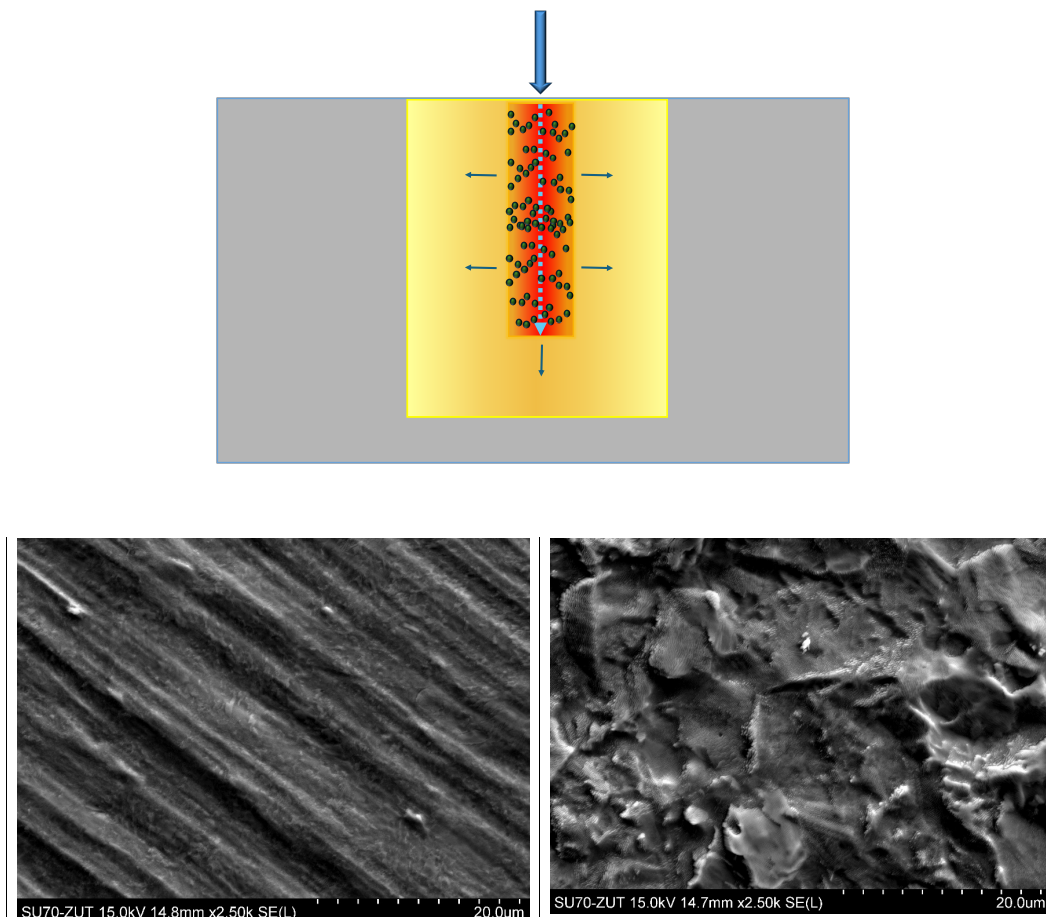


Fig. 4: Top: Illustration of an expanding ion track. Bottom: Scanning electron microscope (SEM) images of the Zr target before (left) and after (right) deuteron irradiation.

In summary, we have presented for the first time a thick-target yield measurement of the ${}^2\text{H}(d,p){}^3\text{H}$ reaction down to the previously unavailable deuteron energy in CMS of 0.625 keV. The electron screening energy of 340 ± 30 eV estimated for the measurement over seven orders of magnitude agrees very well with results of previous experiments and theoretical predictions. At the lowest CMS deuteron energies below 1.25 keV, a thick-target yield plateau has been observed, which is about two orders of magnitude above the presumed contribution of neutralized deuterium ions. The protons emitted in this beam energy region have significantly higher energies than those expected for irradiation with neutral deuterons and can be explained by the DD reactions occurring at thermal (meV) energies. According to calculations, the thermal DD reactions can take place in the ion tracks induced by the deuteron beam, where high phonon densities and temperatures above the melting point can be reached. The model explains both the absolute value of the effect and the observed reaction yield plateau at the lowest projectile energies. The achieved results confirm that DD reactions can take place at thermal energies due to high electron screening energies in the hosting metallic environments and the threshold resonance observed previously. The absolute yield of these effects can be additionally modulated by the number of crystal lattice defects determining the electron screening energy, which opens perspectives for future material and commercial studies.

References

1. Czernski, K. et al. Enhancement of the electron screening effect for d + d fusion reactions in metallic environments, *Europhys. Lett.* **54**, 449-455 (2001).
2. Kasagi, J. et al. Strongly Enhanced Li + D Reaction in Pd Observed in Deuteron Bombardment on PdLi_x with Energies between 30 and 75 keV; *J. Phys. Soc. Jpn.* **73**, 608-612 (2004).
3. J. Cruz et al. Electron screening in ${}^7\text{Li}(p,\alpha)\alpha$ and ${}^6\text{Li}(p,\alpha){}^3\text{He}$ for different environments, *Phys. Lett. B* **624**, 181-185 (2005).
4. Cvetinovic, A. et al. Molecular screening in nuclear reactions, *Phys. Rev. C* **92**, 065801 (2015).
5. Ichimaru, S. Pycnonuclear reactions in dense astrophysical and fusion plasmas, *Physics of Plasmas* **6**, 2649 (1999).
6. Czernski, K. et al. Screening and resonance enhancements of the $2\text{H}(d, p){}^3\text{H}$ reaction yield in metallic environments, *EPL* **113**, 22001 (2016).
7. Kowalska, A. et al. Crystal Lattice Defects in Deuterated Zr in Presence of O and C Impurities Studied by PAS and XRD for Electron Screening Effect, *Materials* **16**, 6255 (2023).
8. Czernski, K. Deuteron-deuteron nuclear reactions at extremely low energies, *Phys. Rev. C* **106**, L011601 (2022).
9. Czernski, K. et al. Indications of electron emission from the deuteron-deuteron threshold resonance, *Phys. Rev. C* **109**, L021601 (2024).
10. Haridas Das, G. et al. High-energy electron measurements with thin Si detectors, *Measurement* **228**, 114392 (2024).
11. Dubey, R. et al. Experimental signatures of a new channel of the DD reaction at very-low energy, arXiv:2408.07567 [nucl-ex] (2024).

12. Kasagi, J. et al. Strongly Enhanced DD Fusion Reaction in Metals Observed for keV D+ Bombardment, *J. Phys. Soc. Jpn.* **71**, 2881 (2002).
13. Huke, A. et al. Enhancement of deuteron-fusion reactions in metals and experimental implications, *Phys. Rev. C* **78**, 015803 (2008).
14. Arai, K. et al. Tensor Force Manifestations in Ab Initio Study of the $^2\text{H}(d,\gamma)^4\text{He}$, $^2\text{H}(d,p)^3\text{H}$, and $^2\text{H}(d,n)^3\text{He}$ Reactions, *Phys. Rev. Lett.* **107**, 132502 (2011).
15. Lindsay, B. G. & Stebbings, R. F. Charge transfer cross sections for energetic neutral atom data analysis, *J. Geophys. Res.* **110**, A12213 (2005).
16. Ziegler, J.F., Biersack J.P. & Littmark, U. *The Stopping and Range of Ions in Solids*, vol. 1 of *The Stopping and Ranges of Ions in Matter*, Pergamon Press, New York, 1985.
17. Kaoumi, D., Motta, A. T. & Birtcher, R. C. A thermal spike model of grain growth under irradiation, *J. App. Phys.* **104**, 073525 (2008).
18. Dufour, C. & Toulemonde, M. Models for the Description of Track Formation, in W. Wesch and E. Wendler (eds.), *Ion Beam Modification of Solids*, Springer Series in Surface Sciences 61, (2016), p. 63-104
19. Giri, A. et al. Electron-phonon coupling and related transport properties of metals and intermetallic alloys from first principles, *Materials Today Physics* **12**, 100175 (2020).
20. Zhang, Y. & Weber, W. J. Ion irradiation and modification: The role of coupled electronic and nuclear energy dissipation and subsequent nonequilibrium processes in materials, *Appl. Phys. Rev.* **7**, 041307 (2020).
21. Olsson, P. A. T. et al. Ab initio thermodynamics of zirconium hydrides and deuterides, *Computational Materials Science* **86**, 211-222 (2014).
22. Long, X. et al. Hydrogen Isotope Effects of Ti, Zr Metals, *Fusion Science and Technology* **60**, 1568-1571 (2011).

Methods

Experimental setup

The experiments were conducted at the eLBRUS Ultra High Vacuum Accelerator of the University of Szczecin, Poland. The facility combines a very good vacuum of 10^{-10} mbar in the target chamber with a high current ion beam up to 1 mA on the target²³. Due to dropping cross sections of nuclear reactions at very low energies below the Coulomb barrier, an important feature of the accelerated ion beams is their very good energy definition of 10 eV and the long-term stability of about 5 eV, provided by the ECR ion source. The accelerated system has been recently upgraded (see Fig. 6) and put on a special platform increasing or decreasing its potential compared to the target chamber at the ground potential. In front of the target chamber a decelerating system consisting of two electric lenses has been additionally installed. Thanks to the modification, the ion source could be operated at high potentials delivering high currents independent of the final beam energies. After deceleration, a beam current of several hundred microamps at the lowest projectile energies of about 1 keV, focused to a 7 mm diameter beam spot on the target could be achieved. The highest acceleration potential is 26 kV.

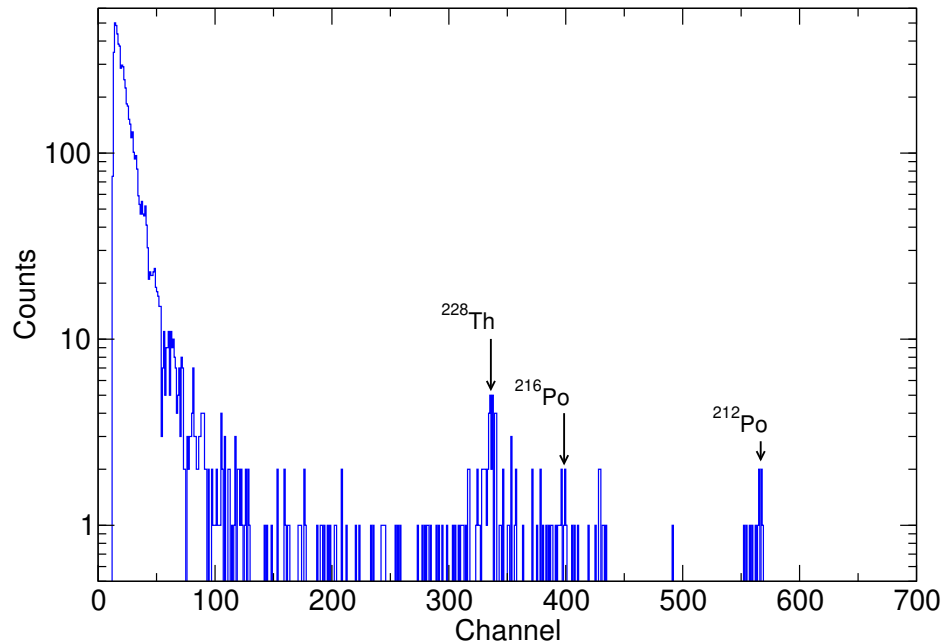


Fig. 5: Natural background spectrum characteristic for the ^{232}Th alpha-decay series: ^{228}Th 5.52 MeV, ^{216}Po 6.91 MeV, ^{212}Po 8.95 MeV. The energies measured are lower than the nominal decay values due to the energy loss of alpha particles in the protection foil in front of the Si detector.

In the present experiment, atomic and molecular deuteron beams D_1^+ , D_2^+ and D_3^+ , analyzed magnetically have been applied. The charged particles emitted in the DD reactions: 0.8 MeV ^3He , 1.02 MeV ^3H and 3 MeV protons have been registered by a low-noise PIPS Si detector (100 μm thick, 100 mm^2 detection area) placed at a distance 7 cm from the target, at an angle of 135° to the beam. In front of the detector, a 1 μm thick aluminum foil has been located to prevent elastically scattered deuterons from entering the detector. As a target, a 1mm thick Zr plate implanted to the highest possible stoichiometry ZrD_2 has been applied. Deuterated Zr targets are known for their high stability and isotropic deuterium density distribution, as well as for their high electron screening energies⁶. Experimental spectra measured at different energies using atomic and molecular deuterium beams are displayed in Fig. 1. The stability of the energy calibration of the Si detector during the long-term measurements at the lowest beam energies was assured by controlling the line position of the natural background dominated by three main alpha-decays (see Fig. 5).

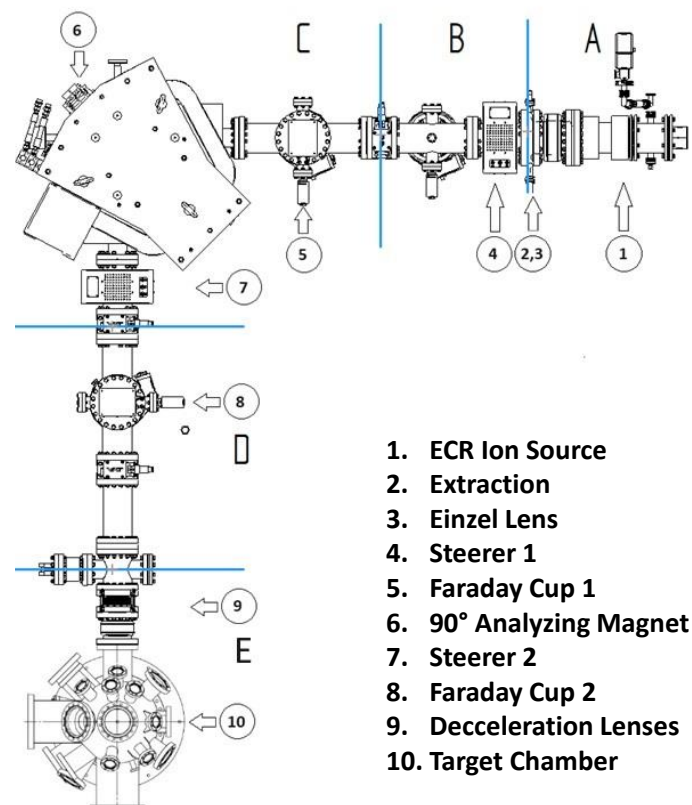


Fig. 5: Ultra-high vacuum accelerator system at the University of Szczecin, Poland. The displayed sections of the system correspond to different units of the differential pumping system.

Despite very good vacuum in the target chamber, the differential pumping system gradually reduces the vacuum pressure at the ion source of 10^{-6} mbar to the value of 5×10^{-9} mbar in the beam line behind the analyzing magnet. Due to increasing cross sections of charge exchange reactions on air and hydrogen molecules for lowering energies, a fraction of the ion

beam can be neutralized in this part of the beam line and is not decelerated by the electric lenses in front of the target chamber. Considering 1 m distance between the electric beam steerer and the deceleration lenses and the neutralization cross section¹⁵ of 10^{-15} cm² at 8×10^{-9} mbar rest gas pressure, the fraction of neutral beam atoms/molecules can be estimated to about 4×10^{-5} . This value is very close to the experimentally determined fractions for D_1^+ and D_2^+ beams of approximately 10^{-4} (see main text and Fig. 2a), which is especially important for measurements of strongly decreasing reaction cross sections.

Thick target yield vs. reaction rate

The screened reaction cross-section below the Coulomb barrier can generally be expressed by the astrophysical S-factor:

$$\sigma_{scr}(E) = \frac{1}{\sqrt{E(E+U_e)}} S(E) \exp\left(-\sqrt{\frac{E_G}{E+U_e}}\right) \quad (7)$$

where the astrophysical S-factor $S(E)$ in absence of narrow resonances is usually a slowly changing function of the CM energy. In the low energy accelerator studies, the cross section cannot be determined directly as the range of projectiles is very low and the cross-section changes strongly. Instead, the thick target yield being a sum of the reaction contributions from different target depth is a standard quantity that can be obtained:

$$Y_{scr}(E) = N_0 \int_0^R \sigma_{scr}(E) dx = N_0 \int_0^E \frac{\sigma_{scr}(E)}{|dE/dx|} dE \quad (8)$$

where the density of reacting nuclei in the target N is assumed to be constant along of the pathway of projectiles up to their range R . The stopping power function $|dE/dx|$ has to components: electronic and nuclear. The electronic part describes energy loss mechanisms related to atomic excitation and ionization which is proportional to \sqrt{E} in the low energy limit. For projectile energies below 1 keV, the nuclear stopping power associated with scattering on lattice atoms begins to dominate. Since the yield function decreases exponentially with lowering energies and our experiments are performed for deuteron energies higher than 1 keV, we can approximate the stopping power value as $|dE/dx| = C\sqrt{E}$, which leads to an expression:

$$Y_{scr}(E) = N_0 \int_0^E \frac{\sigma_{scr}(E)}{C\sqrt{E}} dE = \frac{N_0}{C} \int_0^E \frac{\frac{1}{\sqrt{E(E+U_e)}} S(E) \exp\left(-\sqrt{\frac{E_G}{E+U_e}}\right)}{\sqrt{E}} dE \quad (9)$$

This integral can be calculated analytically:

$$Y_{scr}(E) = \frac{2N_0 S(E)}{c\sqrt{E_G}} \left[\exp\left(-\sqrt{\frac{E_G}{E+U_e}}\right) - \exp\left(-\sqrt{\frac{E_G}{U_e}}\right) \right] \simeq \frac{2N_0 S(E)}{c\sqrt{E_G}} \exp\left(-\sqrt{\frac{E_G}{E+U_e}}\right) \quad (10)$$

assuming that the astrophysical S-factor does not change strongly and that $E \gg U_e$. The S-factor is a coherent sum of a broad resonance contribution S_B and the narrow 0+ threshold resonance^{6,8} S_R :

$$S(E) = S_B + S_R(E) + 2 \left(\frac{1}{3} S_B S_R(E) \right)^{1/2} \cos(\varphi_B^{0+}) \quad (11)$$

where $S_B = 57 \text{ keV b}$ is taken as a constant¹⁴, and only one third of its value contributes to the interference effect. The resonance component can be described by a Breit-Wigner formula:

$$\sigma_R(E) = \frac{\pi}{k^2} \frac{\Gamma_d \Gamma_p}{(E-E_R)^2 + \Gamma^2/4} \simeq \frac{\pi}{k^2} \frac{\Gamma_d \Gamma_p}{E^2} \quad (12)$$

Here we consider $E_R \rightarrow 0$. The deuteron partial width takes the value for the single particle resonance:

$$\Gamma_d(E + U_e) = 2kaP(E + U_e) \frac{\hbar^2}{\mu a^2} = 2k \frac{\hbar^2}{\mu a} (E_G/(E + U_e))^{1/2} \exp[-(E_G/(E + U_e))^{1/2}] \quad (13)$$

and

$$S_R(E) = \frac{(2E_G)^{1/2} \hbar^3 \Gamma_p}{a \mu^{3/2} E^2} \quad (14)$$

Since the resonance contribution to the thick target yield in the energy range studied is relatively low compared to a strong screening enhancement, the screening curves presented in Fig. 2 and 3 do not include resonance contribution and the S-factor was assumed to be constant.

Oppositely to the standard accelerator experiments, where a projectile reacts with resting target nuclei, in the case of the classical plasma at temperature kT , where all the constituents interact with each other, the nuclear reaction rate is a proper quantity to describe the observed number of reactions:

$$\mathcal{R}(T) = \frac{N^2}{2} \langle \sigma v \rangle = \frac{N^2}{2} \frac{(8/\pi)^{1/2}}{\mu^{1/2} (kT)^{3/2}} \int_0^\infty \sigma(E) E \exp(-E/kT) dE \quad (15)$$

Here we assumed the classical Maxwell-Boltzmann velocity distribution. In the case of a narrow Breit-Wigner resonance, considering that its resonance strength is distributed over a small thermal energy spectrum, we get:

$$\mathcal{R}(T) = \frac{N^2}{2} \left(\frac{2\pi}{\mu kT} \right)^{3/2} \hbar^2 \exp(-E_R/kT) \frac{\Gamma_d \Gamma_p}{\Gamma} \quad (16)$$

The expression for the deuteron single-particle resonance width (Eq.13) at $E = 0$ finally leads to:

$$\mathcal{R}(T) = N^2 \frac{16\pi^{3/2} \hbar^3 E^{1/2}}{\mu^2 a (kT)^{3/2}} (E_G/U_e)^{1/2} \exp[-(E_G/U_e)^{1/2}] \exp(-E_R/kT) \frac{\Gamma_p}{\Gamma} \quad (17)$$

The screening function $\exp[-(E_G/U_e)^{1/2}]$ is the main factor deciding on the absolute value of the reaction rate. However, the number density N strongly depends on the temperature, as well. Its value can be correlated to the diffusion coefficient and can be expressed as $N = N_0 \exp(-E_A/kT)$, where E_A denotes the activation energy, equal to 413 meV for ZrD_2 ²². The local temperature within the ion track induced by bombarding deuterons is related to a number of excited phonons described by the well-known nuclear stopping power function¹⁶. The maximum of the nuclear stopping power for the ZrD_2 target is at 80 eV, which is much higher than for pure metallic Zr of 1.5 keV, which results in higher phonon density and ion track temperature (see Fig. 3).

References

23. M. Kaczmarek, et al. New accelerator facility for measurements of nuclear reactions at energies below 1 keV, *Acta Phys. Pol. B* **45**, 509 (2014).
24. Czerski, K. et al. The $^2H(d,p)^3H$ reaction in metallic media at very low energies, *Europhys. Lett.* **68**, 363 (2004).